



MAXIMIZING UAV RANGE THROUGH WING AEROSTRUCTURAL OPTIMIZATION: A STUDY ON CHORD, SHAPE, SPAN AND COMPOSITE MATERIAL PROPERTIES

CARDOSO, PEDRO M. (1); MARTA, ANDRÉ C.(2); MATOS, NUNO M. (3)

(1) IDMEC, IST, U.LISBOA, E-mail: pedro.marques.cardoso@tecnico.ulisboa.pt

(2) IDMEC, IST, U.LISBOA, E-mail: andre.marta@tecnico.ulisboa.pt

(3) TEKEVER UAS, E-mail: nuno.matos@tekever.pt

RESUMO

No mercado competitivo de UAV, os fabricantes esforçam-se por melhorar o desempenho através de tecnologias de design avançadas. Este estudo centra-se na maximização do alcance de um UAV através da utilização de otimização baseada em gradientes que acopla alta fidelidade de Dinâmica de Fluido e Estrutural Computacional. O processo de otimização considera variáveis aerodinâmicas e estruturais de projeto, nomeadamente a corda, perfil alar, envergadura, espessura da estrutura e orientação da fibra do material composto. O método adjunto discreto é utilizado para calcular os derivados de forma eficiente para um grande número de variáveis permitindo otimização baseada em gradientes. Os resultados demonstram um aumento de até 9,9% no intervalo, uma melhoria de 32% na eficiência aerodinâmica, apesar de um aumento de 114% no peso da asa. A abordagem de disciplinas aerodinâmicas e estruturais oferece, simultaneamente, informações valiosas sobre os compromissos entre diferentes variáveis de design e leva a projetos de UAV mais eficientes.

Palavras-chave: otimização multidisciplinar, design de aeronaves, método adjunto, deformação de forma livre, materiais compósitos.

ABSTRACT

In the competitive UAV market, manufacturers strive to enhance performance through advanced design technologies. This study focuses on maximizing the range of a UAV through the use of a gradient-based optimization framework that couples high-fidelity Computational Fluid Dynamics and Computational Structural Dynamics models. The optimization process considers aerodynamic and structural wing design variables (DV), namely chord, airfoil shape and span, panel thickness and fiber orientation of the constitutive composite material. The discrete adjoint method is used to compute derivatives efficiently for a large number of DV and gradient-based optimization. The results demonstrate up to 9.9% increase in range, a 32% improvement in aerodynamic

efficiency, despite a 114% increase in wing weight. Addressing both aerodynamic and structural disciplines concurrently offers valuable insights into the trade-offs among different design variables and leads to more efficient UAV designs.

Keywords: multidisciplinary optimization, aircraft design, adjoint method, free-form deformation, composite materials.

1 INTRODUCTION

In recent years, the landscape of unmanned aerial vehicles (UAVs) has evolved rapidly, with the global fixed wing drone market, estimated at \$8.3 billion USD in 2023. With an expected Compound Annual Growth Rate (CAGR) ranging from 8.3% to 17.2% (1), the competition among UAV manufacturers is increasingly fierce. This focuses is on the enhancement of the TEKEVER AR5 to strengthen its competitive edge in the Medium-Altitude Medium-Endurance (MAME) fixed-wing UAV sector (Figure 1).

Figure 1: TEKEVER AR5 (source: TEKEVER UAS)



This UAV model is designed to execute a variety of missions, including search and rescue, maritime surveillance, and maritime patrol, offering advantages such as extended endurance and cost-effective operation. A summary of its key specifications is provided in Table 1.

Table 1: TEKEVER AR5 characteristics (source: TEKEVER UAS)

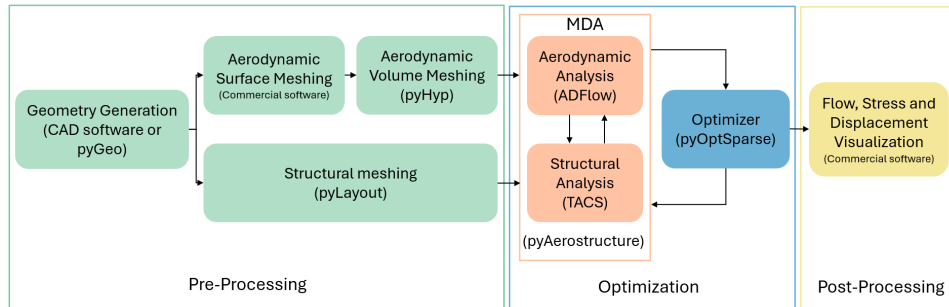
Cruise speed	Cruise altitude	Payload	Wing span	Wing area	Length	Endurance
100 km/h	340 m	50 kg	7.3 m	4.36 m ²	4 m	20 h

The primary objective is to improve the wing of the AR5, enhancing its aerodynamic efficiency and structural integrity. Considering that the wing is a flexible structure, whose shape differs significantly under loads in flight due to fluid-structure interactions, a high-fidelity aerostructural design tool is employed (3). This study is a follow up of the work done in (4), where the wing twist and the effect of maintainability constraints was analyzed, being know tested the effect of additional aerodynamic Design Variables (DV), namely chord, span and airfoil shape. Furthermore, it was previously demonstrated that there is a strong coupling between the structural and aerodynamic behavior of the TEKEVER AR5 wing that will benefit from this more complex and time consuming optimization.

2 AEROSTRUCTURAL DESIGN FRAMEWORK

The aerostructural design framework used is MACH-Aero, developed by the Multidisciplinary Design Optimization (MDO) Laboratory at the University of Michigan. It includes three main stages, as depicted in Figure 2.

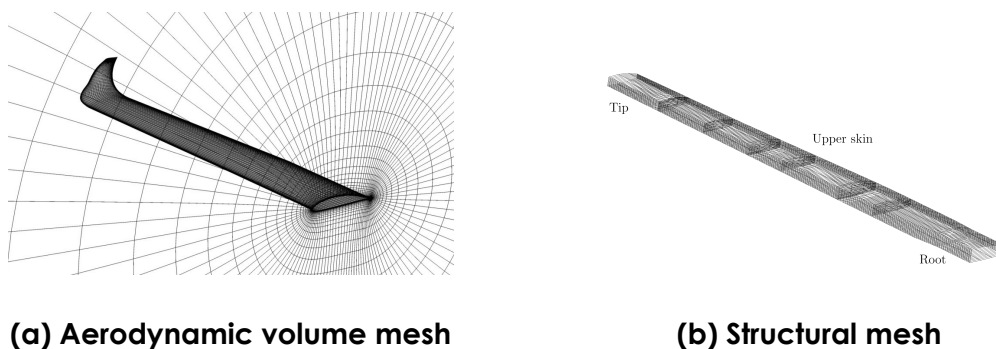
Figure 2: Aerostructural design framework (3)



2.1 Pre-processing stage

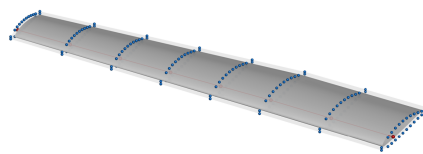
Based on the geometry CAD description of the TEKEVER AR5 wing, the aerodynamic mesh is created. Starting by the creation of surface mesh characterized by its high density at the leading, trailing edge and wing tip (4) and sharp edges are avoidance consistent with being a based for hyperbolic strutted volume mesh. The next step is the volume mesh generation using `pyHyp` (5), achieving the general topology observed in Figure 3a, which also applies the far-field and wall boundary conditions. The first layer height was prescribed, and latter verified to guarantee a y^+ close to unity as required by the Spalart-Allmaras turbulence model employed, chosen for its effectiveness at predicting the turbulent effect around the wing at the AR5 operating conditions and for being differentiated in the Mach-Aero framework (6). A mesh refinement study concluded that 800,000 cells were sufficient, considering the trade-off between accuracy and performance, with 0.5% difference in lift and 5% drag but converged in only 20% of the time, compared to the most refined mesh studied. The computational domain extends 20 chords.

Figure 3: Computational meshes of TEKEVER AR5 wing (3)



To avoid the computational burden of generating new meshes from scratch, the Free-Form Deformation (FFD) method (7) is employed, which is based on generating boxes through control points surrounding the wing surface (as shown in Figure 4), then when moved modify the wing geometry (8). Although each of the points can be individually moved, as is done in airfoil shape optimization, it is more practical to reduce and create more recognizable DV. Therefore, they are aggregated as parametric global variables like chord, twist, and span (8). In Mach-Aero, `pyGeo` is the module responsible for performing this task; moreover, it also handles the computation of the global DV derivatives using the chain rule, starting from the already computed derivative of the movement of each individual point (8).

Figure 4: Free form deformation (FFD) box (3)



The structural finite element mesh is generated with `pyLayout`, an automated module for the creation of wingbox structures for wings. When given a CAD file along with the position of spars and ribs generates the structural layout, as shown in Figure 3b. Since these wing parts are thin and made of fibre-reinforced composite materials, bilinear, 4-node, 2-D shell elements were used (9). From a mesh convergence study monitoring the tip displacement and average stress, a mesh with 1,000,000 DoF was selected, which presents an error smaller than 2% in both parameters.

2.2 Optimization stage

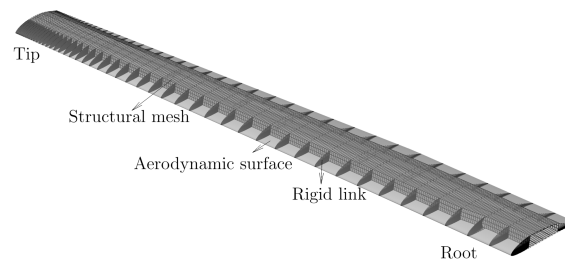
The Multidisciplinary Feasible (MDF) MDO architecture is used for its simplicity and accuracy at the optimizer level (10, 2). The problem is solved as a single discipline where the couple results are given by a Multidisciplinary Analysis (MDA). This methodology is used as it allows for the use of the previously developed, fully differentiated aerodynamic and structural solvers (11). The aerodynamic discipline is solved using `ADFLOW` (12) and the structural discipline is solved using `TACS` (13). Both solvers have the ability of computing DV linked to them, namely, flow properties, wing aerodynamic shape, material fiber orientation and thickness.

`ADFLOW` employs a finite-volume method to solve the steady compressible RANS equations, utilizing the Spalart-Allmaras model for turbulence. The models' discretization relies on central finite differences with JST scalar dissipation. As `ADFLOW` is a compressible flow solver and the `TEKEVER AR5` operates at very low Mach number, the solver uses characteristic time-stepping combined with an approximate Newton method, and the van Leer-Lee-Roe preconditioner to enhance both accuracy and convergence. Convergence is defined by achieving a 10^{-6} reduction in the L2-norm of the residual. Default settings are used for all other solver settings (12).

`TACS` is finite-element solver and computes the generalized Hooke's Law (14,

9). The material is considered orthotropic, with the fibres parallel within a ply, allowing the rule of mixtures (15). The failure criteria is the Tsai-Wu (16). The disciplines are coupled using `pyAerostructure`, which captures the interactions between aerodynamic forces and structural displacements (2). The MDA is converged using Gauss-Seidel, a fixed-point method in which each discipline analysis is run using the most recent output from the other disciplines until a consistent set of state variables is returned. The MDA convergence tolerance was set to 10^{-5} . The displacements are transferred between the meshes through using the Rigid Link Transfer (RLT) technique (2) (Figure 5), and the method of virtual work is used to determine the structural nodal forces (17, 2) given by the integration of the aerodynamic loads.

Figure 5: Overlay of the rigid links, structural and aerodynamic mesh(3)



The wing volume mesh is deformed at each aerostructural iteration during using an Inverse-Distance Weighting method (IDW) (5).

The gradient-based SLSQP algorithm is used in the optimization process itself, that proved to be adequate in similar problems (18). The module `pyOptSparse` (19) implements such constrained optimizer.

The sensitivity analysis, required for the search direction evaluation in the gradient-based optimizer, is efficiently and accurately performed using the adjoint method, since there are considerably more design variables than metric functions (20). The coupled system of adjoint equations is treated as a unified problem, solving the entire set together to directly address the interdependencies between different disciplines, leading to more accurate sensitivity analysis and faster convergence (2). The adjoint solver is converged using the Krylov subspace approach, with a tolerance of 10^{-5} .

To prevent material failure, the Kreisselmeier-Steinhauser (KS) aggregation technique is used (9), which provides a smooth estimate of the maximum stress, while avoiding issues of discontinuity and excessive constraints.

3 TEKEVER AR5 MULTIDISCIPLINARY OPTIMIZATION

The aerostructural optimization targets the maximization of the aircraft range R defined by the Breguet equation,

$$R = \frac{L}{D} \frac{\eta}{sfc \cdot g} \ln \left(\frac{W_0}{W_f} \right), \quad (1)$$

where the lift L and drag D coefficients depend on the aerodynamic performance, and the initial W_0 and final W_f weight depend on the structural

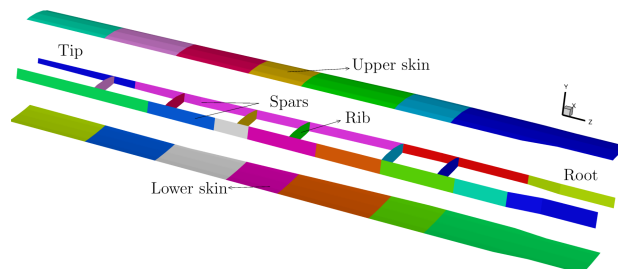
performance, the remaining equation terms are fixed by flight operating condition, the propulsion efficiency η and specific fuel consumption sfc . g is the gravitational acceleration. Finally, the wing design variables (DV) are summarized in Table 2.

Table 2: Design variables

Design variable	Description	Quantity	Lower bound	Upper bound
α	angle of attack	1	-4°	20°
γ	twist distribution	7	-15°	15°
c	chord distribution	7	-1 m	1.5 m
b	span	7	1 m	1.5 m
$shape$	shape	6x8	-0.05 m	0.05 m
θ_1/θ_2	fibre angle	2N	0°	90°
t	material thickness	N	0.01 m	0.1 m

The twist and chord distributions are functions of the wing spanwise coordinate (see Figure 4). The shape DV is controlled by 6 points along the airfoil, along 7 section in the spanwise direction (see Figure 4), where each of the control points has the freedom to move up and down, inside its bounds, changing the airfoil shape. The fibre angles and material thickness are defined for each block i of the N blocks presented in Figure 6.

Figure 6: Wing structural design variables by blocks (3)



The design must satisfy five requirements, included in the form of constraints in the optimization: i) the aircraft trimming implies that the lift generated must match the UAV weight at level flight, $L = W$; the structure must not fail under a 2-g manoeuvre, $KS(failure) \leq n(2g)$; iii) adjacency constraints to keep the difference in each design block thickness under a maximum threshold, $|t_i - t_{i+1}| \leq \Delta_{max}$; iv) composite ply angle continuity among consecutive blocks for manufacturability, $\theta_{1,i} = \theta_{1,i+1}$ and $\theta_{2,i} = \theta_{2,i+1}$; and v) orthogonality between plies for manufacturability to allow the use of carbon fibre cloths with weaving pattern, $|\theta_1 - \theta_2| = 90^\circ$. In (3), the impact of adding these manufacturability constraints was analyzed. It was concluded that while they do not significantly affect the final optimal result, they greatly enhance the wing's manufacturability (3). Moreover, despite existing the capability of aerostructurally analyze all corners of V-n diagram (velocity vs load factor) with linear structural response, it was decided to only consider maximum load maneuvering and level flight, to save on computational effort. The wing aerostructural design problem can be written in standard optimization form as

$$\begin{aligned}
& \text{maximize} && R \\
& \text{with respect to} && \alpha, c, b, \text{shape}, \theta_{1,i}, \theta_{2,i}, t_i \\
& \text{subject to} && L = W \\
& && KS(\text{failure}) \leq n(2g) \\
& && |t_i - t_{i+1}| \leq \Delta_{\max} \\
& && \theta_{1,i} = \theta_{1,i+1} \\
& && \theta_{2,i} = \theta_{2,i+1} \\
& && |\theta_1 - \theta_2| = 90^\circ.
\end{aligned} \tag{2}$$

The summarized results of the optimization using the simplified TEKEVER AR5 wing as the starting geometry are found in Table 3. As previously mentioned, the structural constraints have already been studied, so this study focuses on the impact of adding different aerodynamic DVs. Throughout the study, all structural DVs are included, along with the angle of attack.

Table 3: Design variables

Case	Wing mass, kg (wing)	L/D (wing)	Range, m (UAV)
Starting geometry	ref	ref	ref
Twist distribution (3)	-50%	+0.6%	+0.9%
Chord distribution	-56%	-1.2%	+1%
Span + Twist distribution	+130%	+20%	+6.3%
Airfoil shape	-42%	+10.56%	+4.53%
All	+114%	+32%	+9.9%

It can be concluded that an aerostructural optimization of the TEKEVER AR5 wing yields significant improvements in the UAV range. The aerostructural approach allows for an automatic trade-off between design variables that directly affect both disciplines, such as the aircraft's wingspan. Indeed, this solution would not be possible in a single-discipline optimization, highlighting it as one of the best options available. Furthermore, the objective function, which considers both aerodynamic and structural concerns, ensures that no single adverse outcome (such as an increase in mass or a decrease in aerodynamic efficiency) led to a reduction in range showcasing the couple performance behavior. The results also show that when more freedom is given to the optimizer, such as in shape optimization and with all design variables included, significantly better outcomes can be achieved. A detailed discussion of the new cases is included next.

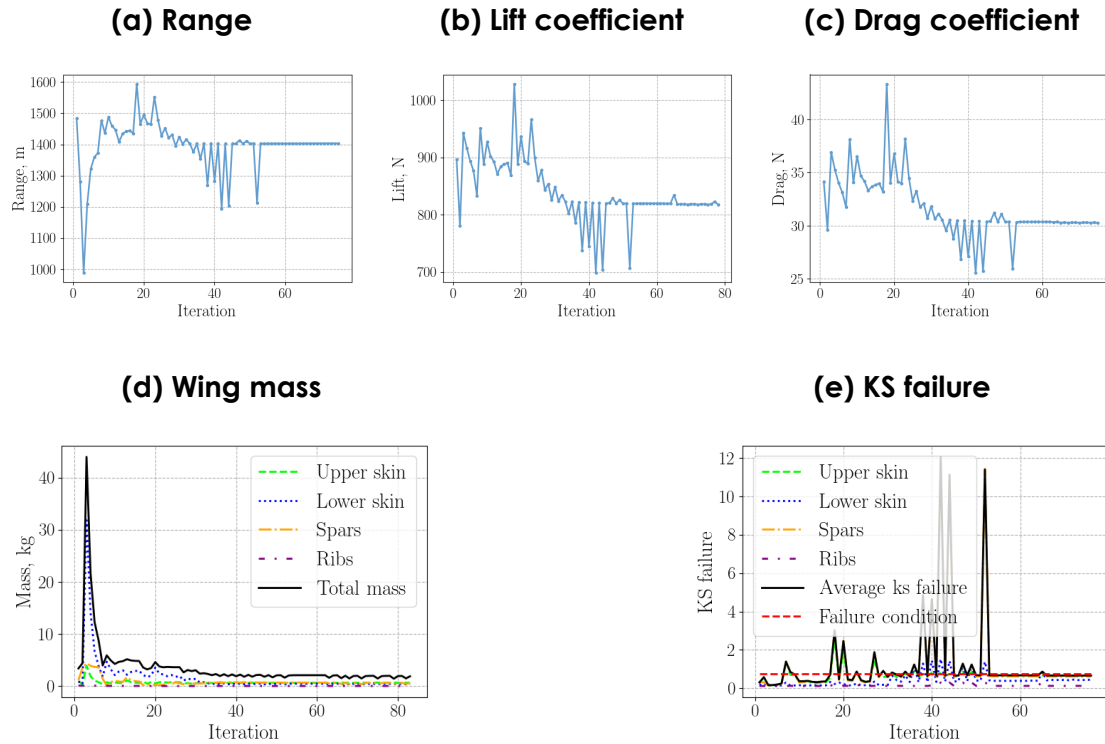
3.1 Chord optimization

Starting from the simplified TEKEVER AR5 wing design without winglet, a first optimization was done considering the chord distribution and angle-of-attack as design variables. Overall, a 0.9% increase in range was achieved, following a 56% decrease in wing mass due to the smaller skin panels and the thinner walls, despite a 1.2% decrease in aerodynamic efficiency.

Figure 7 shows the optimization convergence history of five key parameters in 93 iterations. It is clear the need for less lift for trimming (Fig.7b), the reduction in drag (Fig.7c) by reducing the lift needed and the overall wetted

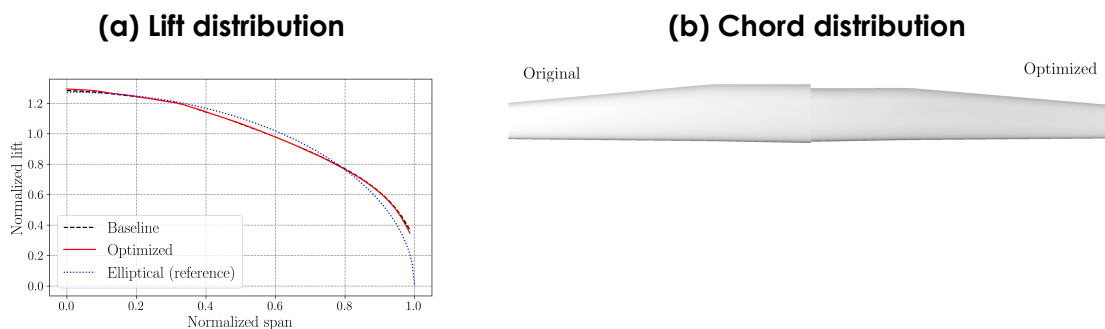
area, and the search for a lighter structure (Fig.7d) while avoiding structural failure (Fig.7e).

Figure 7: Optimization history of key parameters



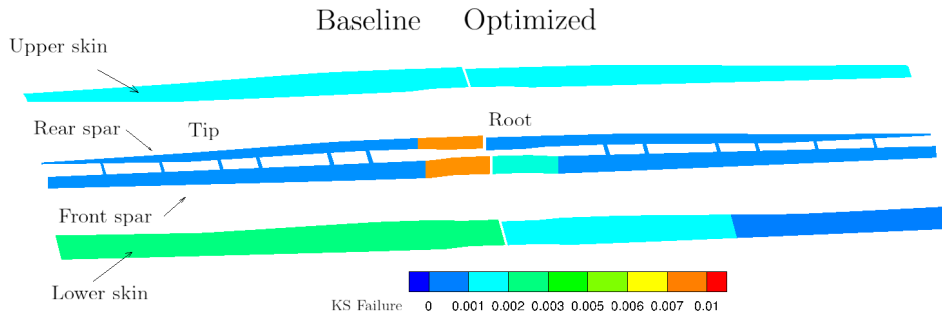
The optimal chord and lift distributions are illustrated in Figure 8a and Figure 8b, respectively. As expected, the optimizer did not converge on the ideal aerodynamic solution (elliptical lift distribution). Instead, it produced a slight increase in lift near the wing root and a reduction near the tip for more efficient structural loading. However, the primary achievement that contributed to the increase in range was the reduction in weight, which was the strategy explored by the optimizer. With weight reduction, less lift was needed, and therefore, less wing area was required, which further contributed to the weight reduction.

Figure 8: Aerodynamic spanwise distributions



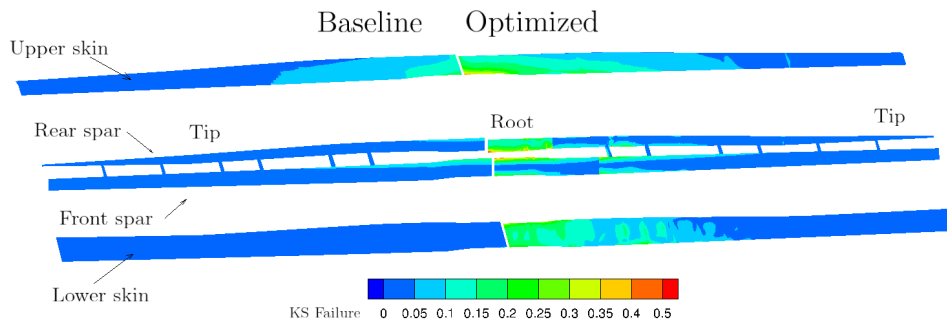
This case led to a significant thinning of the wing panels, as observed in Figure 9, particularly at the front spar and lower skin. As a consequence, a 63% wing weight reduction was achieved.

Figure 9: Thickness distribution



The drastic improvement of the structural efficiency is attested by the KS index failure increase shown in Figure 10, where the optimized wing box exhibits more regions with a higher failure index, meaning it works closer to failure due to the overall thickness decrease.

Figure 10: KS failure index



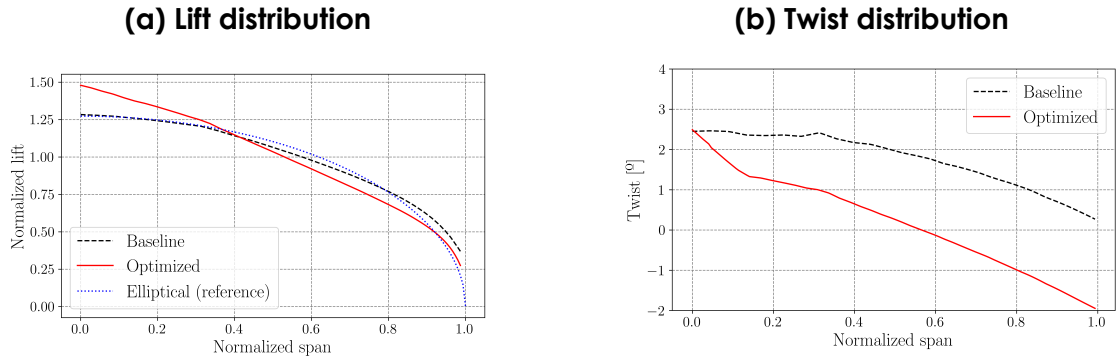
The ply angle distribution in the optimal solution is feasible in terms of manufacturing, being this solution much easier to implement with its orthogonal plies and consistency in ply angles.

3.2 Twist and span optimization

The optimal twist and span optimization was thought to be interesting to address as the aerostructural trade-off between the size of the wing and its structural weight is automatically done. The optimizer converged after 282 iterations, with similar history behavior to that of the previous case.

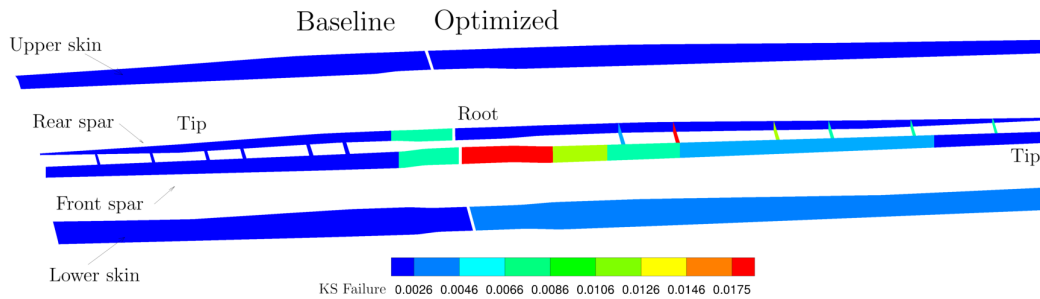
Again, the optimizer did not converge for the ideal aerodynamic solution (elliptical lift distribution) but it drastically increased the lift produced in the wing section closer to the root and reduced it closer to the tip, contributing to a more efficient structural loading (less bending moment, thus lighter structure) and better aerostructural result, as illustrated in Figure 11.

Figure 11: Aerodynamic spanwise distributions



This case led to a 78% increase in span, which improved the aerodynamic characteristics of the wing, namely a 20% increase in lift-to-drag ratio. It is important to mention that this change would impose negative effects in manufacturability costs (material, labor and tools) and logistics of operation with the UAV transport and runway characteristics being harder to accomplish, affecting potential buyers. Due to the increase in span, a thickening of panels was observed (see Figure 12), particularly at the rear spar and lower skin panels near the root, leading to a 130% weight increase.

Figure 12: Thickness distribution

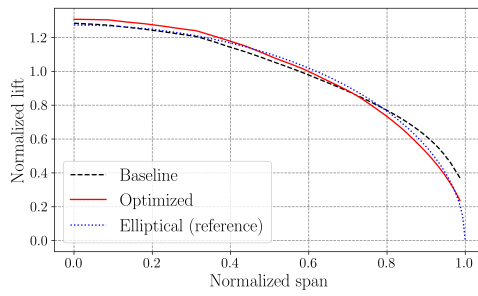


Despite that, the structural efficiency of the wing increased as attested by the increase in the KS index failure that was observed in all the wing structure. The optimized wing box has more regions with a higher failure index, meaning it works closer to failure due to the overall thickness decrease in the tip, despite the general increase in the root.

3.3 Airfoil shape optimization

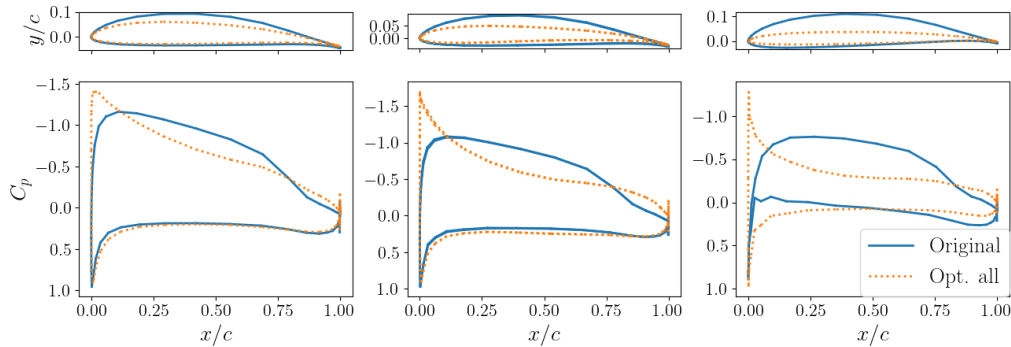
The airfoil shape optimization achieved a 4.5% increase in range, following a 10.5% increase in aerodynamic efficiency and 42% decrease in weight. This time the optimizer took 394 iterations to converge as a result of a larger design space (more DVs). As illustrated in Figure 13, the optimizer converged to a lift distribution close to the ideal aerodynamic solution, but a slight maximum in lift near the wing root and a reduction near the tip is visible for more efficient structural loading and overall performance.

Figure 13: Lift distribution



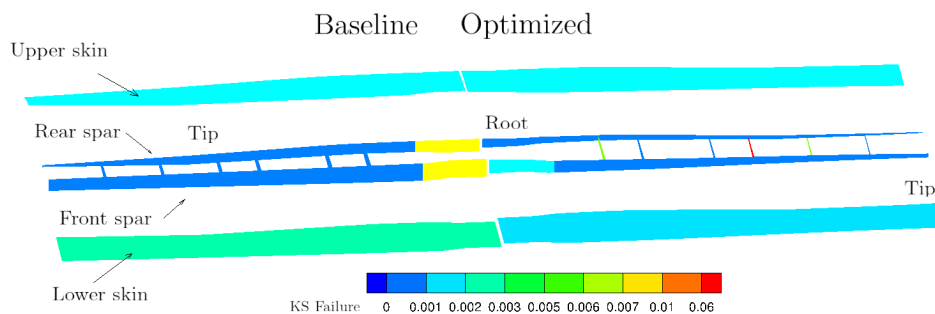
The airfoil shape can be observed in Figure 14, where the capability of the aerostructural analysis is showcased with the trade-off between reducing airfoil thickness for aerodynamic purposes and increasing it for structural ones. Indeed, the optimizer opted for decreasing the original thickness as much as the structure was still able to cope with the loads.

Figure 14: Airfoil shape and coefficient of pressure distribution at 10%, 50% and 90% of the span



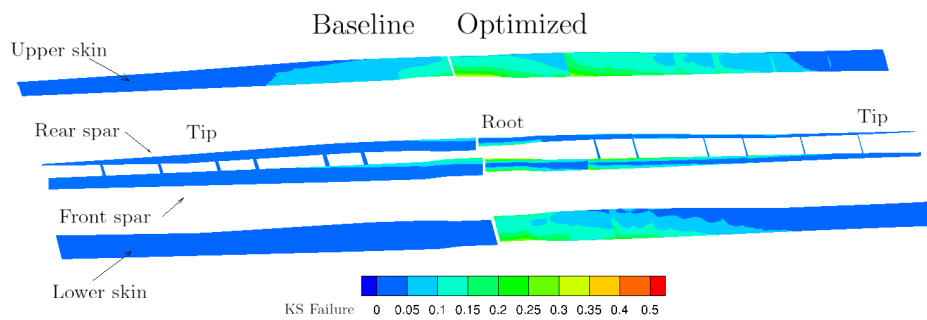
This case led also to an improvement of the structural efficiency as attested by the increase in the KS index failure (Fig.16 due to reduction in panels thickness and the thinning of the airfoil (Fig.15). As a consequence, a 63% wing weight reduction was achieved.

Figure 15: Thickness distribution



It is important to mention that all manufacturability constraints were also respected in this case.

Figure 16: KS failure index

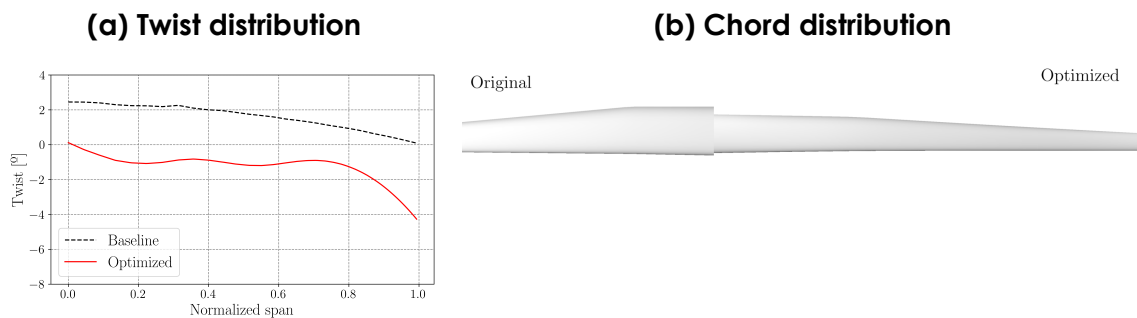


3.4 All design variables

As expected, considering all DV led to the best overall design, with 9.9% range increase, which resulted from a 32% improvement in aerodynamic efficiency, despite a 114% increase in wing weight. This optimization case was by far the most costly, requiring 500 iterations to converge.

The final solution is characterized by operating at an angle-of-attack of 3.14° , with 2.2 times larger span than the baseline wing. The optimal twist and chord distributions are shown in Figure 17, where it is observed an attempt to maximize span, introduce wash-out (negative twist), and reducing the chord to reduce drag, until the increase in structural weight mitigated the effect.

Figure 17: Aerodynamic spanwise distributions



The airfoil shape and pressure distribution, depicted in Figure 18, shown an increase in thickness-to-height ratio, that overcomes the reduction in span, so that sufficient bending stiffness is still obtained.

Once again, the wing lift distribution achieved, shown in Figure 19, produces a more efficient structural loading, with increased lift closer to the root and decreased at the tip.

The optimized wing box has more regions with high failure index, meaning it works closer to failure, as shown in Figure 20, despite the increase in thickness due to the higher bending moments resulting from the larger span, as shown in Figure 21.

The ply angle distribution between the blocks is shown in Table 4 which

Figure 18: Airfoil shape and coefficient of pressure distribution at 10%, 50% and 90% of the span

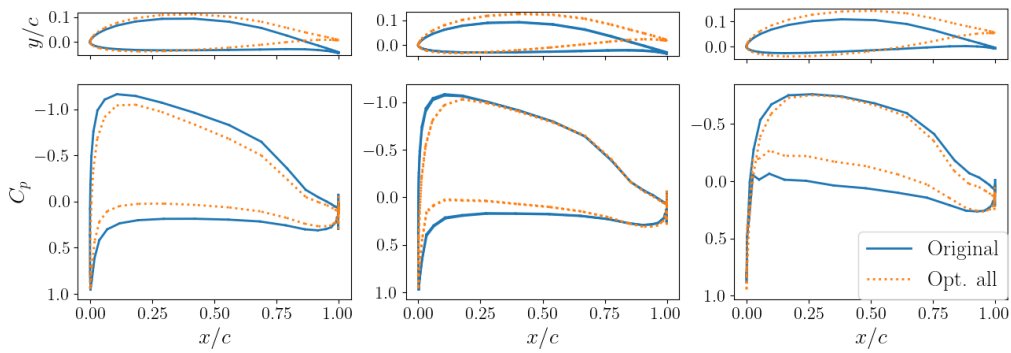


Figure 19: Lift distribution

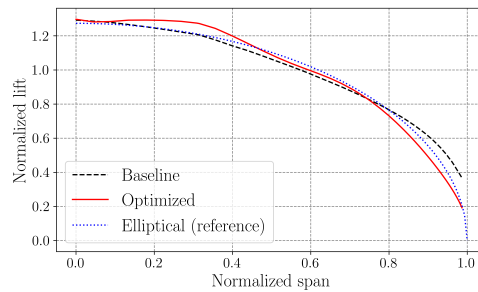


Figure 20: KS failure index

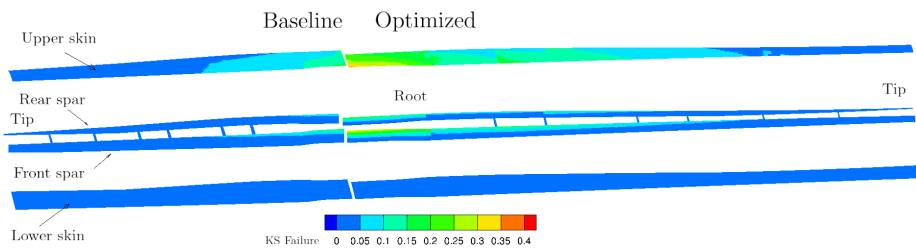
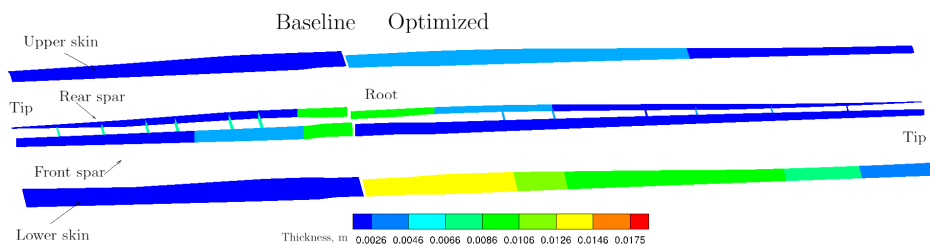


Figure 21: Thickness distribution



demonstrates that the optimal solution is feasible in terms of manufacturing. It is important to mention that the initial configuration in all panel θ_1 is 90° and θ_2 is 0° .

This was the best case solution, indicating that the aggregation of chord, shape and span as DV have room to be improved within the optimization.

Table 4: Ply angles

	Front spar	Rear spar	Upper skin	Lower skin
θ_1	89.6 °	89.8 °	88	89
θ_2	0.4 °	0.2 °	2 °	1 °

4 CONCLUSIONS

High-fidelity MDO has proven to be a powerful tool for aerostructural wing design, achieving an optimal coupled solution by maximizing wing performance for cruise while also analyzing it under a 2g load to ensure structural efficiency during maneuvers. Future work will apply this framework in the detailed design of the next-generation UAV, considering wing shape, structural model, and fuselage effects.

Gains in the TEKEVER AR5 range of +10% were achieved by tweaking all design variables, resulting in a +32% lift-to-drag ratio improvement, despite a 114% wing weight increase due to wingspan growth, thicker shell panels near the root, and adjusted composite ply angles. Although this is the best solution, it requires a costly full wing redesign due to the new wingspan, also potentiality raising production costs from materials, wing molds, and labor; transportation and takeoff logistics become more complex, necessitating larger storage space and impacting potential buyers. A better option is the shape optimization case, yielding a 4.5% range increase from a 42% weight reduction and a 20% lift-to-drag ratio improvement with minimal changes to UAV characteristics, making it suitable for an updated model.

5 ACKNOWLEDGMENTS

This work was supported by Fundação para a Ciência e a Tecnologia (FCT) through IDMEC, under LAETA (project no. UIDB/50022/2024). The authors also acknowledge Tekever UAS for its financial and technical support.

REFERENCES

- 1 Fact.MR, "Fixed Wing Drone Market," 2022. Accessed on 10-09-2023.
- 2 G. K. W. Kenway, G. J. Kennedy, and J. R. R. A. Martins, "Scalable parallel approach for high-fidelity steady-state aeroelastic analysis and adjoint derivative computations," *AIAA Journal*, vol. 52, no. 5, 2014. doi:10.2514/1.J052255.
- 3 A. C. M. Pedro M. Cardoso and N. B. Matos, "Aerostructural design of a medium-altitude medium-endurance fixed wing uav," in *ECCOMAS Congress 2024 - 9th European Congress on Computational Methods in Applied Sciences and Engineering*, (Lisbon, Portugal), 2024.
- 4 R. Gameniro, "Wing Aerodynamic Design for a MAME UAV using High-Fidelity Numerical Tools," Master's thesis, Instituto Superior Técnico, 2023.
- 5 N. R. Secco, G. K. W. Kenway, P. He, C. Mader, and J. R. R. A. Martins, "Efficient mesh generation and deformation for aerodynamic shape optimization," *AIAA Journal*, vol. 59, no. 4, pp. 1151–1168, 2021.

- 6 G. K. Kenway, C. A. Mader, P. He, and J. R. Martins, "Effective adjoint approaches for computational fluid dynamics," *Progress in Aerospace Sciences*, vol. 110, 2019.
- 7 T. W. Sederberg and S. R. Parry, "Free-form deformation of solid geometric models," in *SIGGRAPH '86: Proceedings of the 13th Annual Conference on Computer Graphics and Interactive Techniques*, (New York, USA), Aug. 1986. doi:10.1145/15922.15903.
- 8 G. Kenway, G. Kennedy, and J. Martins, "A cad-free approach to high-fidelity aerostructural optimization," 09 2010.
- 9 G. Kennedy and J. Martins, "A parallel finite-element framework for large-scale gradient-based design optimization of high-performance structures," *Finite Elements in Analysis and Design*, vol. 87, p. 56–73, 09 2014.
- 10 A. C. Gray and J. R. Martins, "Geometrically nonlinear high-fidelity aerostructural optimization for highly flexible wings," in *AIAA Scitech 2021 Forum*, (Virtual event), Jan. 2021. doi:10.2514/6.2021-0283.
- 11 R. Perez, H. Liu, and K. Behdinan, "Evaluation of multidisciplinary optimization approaches for aircraft conceptual design," in *10th AIAA/ISSMO multidisciplinary analysis and optimization conference*, (Albany, USA), Aug. 2004. doi:10.2514/6.2004-4537.
- 12 MDO Lab of University of Michigan, "ADFlow Documentation." <<https://mdolab-adflow.readthedocs-hosted.com>>, 2024. (accessed on 2024-04-03).
- 13 G. J. Kennedy and J. R. Martins, "A parallel finite-element framework for large-scale gradient-based design optimization of high-performance structures," *Finite Elements in Analysis and Design*, vol. 87, 2014. doi:10.1016/j.finel.2014.04.011.
- 14 J. N. Reddy, *Mechanics of Laminated Composite Plates and Shells: Theory and Analysis*. CRC Press, 2nd ed., 2003. doi:10.1201/b12409.
- 15 D. R. Askeland, P. P. Fulay, and W. J. Wright, *The Science and Engineering of Materials*. Cengage Learning, 6th ed., 2010. ISBN:9780495296027.
- 16 A. Khani, S. T. IJsselmuiden, M. M. Abdalla, and Z. Gürdal, "Design of variable stiffness panels for maximum strength using lamination parameters," *Composites Part B Engineering*, vol. 42, no. 3, 2011. doi:10.1016/j.compositesb.2010.11.005.
- 17 G. J. Kennedy and J. R. R. A. Martins, "Parallel solution methods for aerostructural analysis and design optimization," in *Proceedings of the 13th AIAA/ISSMO Multidisciplinary Analysis Optimization Conference*, (Fort Worth, USA), Sept. 2010. doi:10.2514/6.2010-9308.
- 18 Z. Lyu, Z. Xu, and J. R. R. A. Martins, "Benchmarking optimization algorithms for wing aerodynamic design optimization," in *Proceedings of the 8th International Conference on Computational Fluid Dynamics*, (Chengdu, China), July 2014. ICCFD8-2014-0203.
- 19 E. Wu, G. Kenway, C. A. Mader, J. Jasa, and J. R. R. A. Martins, "pyoptspare: A python framework for large-scale constrained nonlinear optimization of sparse systems," *Journal of Open Source Software*, vol. 5, no. 54, p. 2564, 2020.
- 20 J. R. R. A. Martins and G. Kennedy, "Enabling large-scale multidisciplinary design optimization through adjoint sensitivity analysis," *Structural and Multidisciplinary Optimization*, vol. 64, 2021. 10.1007/s00158-021-03067-y.